

## Possible Color Entanglement Effects in p+p and p+A Collisions

---

**Michael J. Skoby\***

*University of Michigan*

*E-mail:* [mskoby@umich.edu](mailto:mskoby@umich.edu)

Due to the non-Abelian nature of QCD, there is a prediction that quarks can become correlated across colliding protons in hadron production processes sensitive to nonperturbative transverse momentum effects. Measuring the evolution of nonperturbative transverse momentum widths as a function of the hard interaction scale can help distinguish these effects from other possibilities. Collins-Soper-Sterman evolution comes directly from the proof of transverse-momentum-dependent (TMD) factorization for processes such as Drell-Yan, semi-inclusive deep-inelastic scattering, and e+e- annihilation and predicts nonperturbative momentum widths to increase with hard scale. Experimental results from proton-proton and proton-nucleus collisions, in which TMD factorization is predicted to be broken, will be presented. The results show that these widths decrease with hard scale, suggesting possible TMD factorization breaking and color entanglement of partons across colliding protons.

*25th International Workshop on Deep Inelastic Scattering and Related Topics*

*3-7 April 2017*

*University of Birmingham, Birmingham, UK*

---

\*Speaker.

## 1. Introduction

Due to the non-Abelian nature of QCD, Rogers and Mulders [1] predicted that quarks can become correlated across colliding protons in hadron production processes sensitive to nonperturbative transverse momentum effects. Rather than two factorized parton distribution functions, correlated partons across protons would be described by a single nonperturbative correlation function. Measuring the evolution of nonperturbative transverse momentum widths as a function of the hard interaction scale can help distinguish these effects from other possibilities. Collins-Soper-Sterman (CSS) evolution comes directly from the proof of TMD factorization and predicts nonperturbative momentum widths to increase with hard scale. Data from Drell-Yan and SIDIS have provided experimental and phenomenological confirmation of this prediction; see e.g. Refs. [2, 3, 4].

The analysis procedure used in this presentation is directly from [5]. The observables used in this analysis are  $\pi^0$ -hadron and  $\gamma$ -hadron correlations, which are sensitive to nonperturbative transverse momentum in the initial state (in the proton) and the final state (hadronization). Figure 1 schematically depicts the  $\pi^0$ -hadron (left) and  $\gamma$ -hadron (right) correlations, where  $p_T^{trig}$  is the trigger particle's transverse momentum,  $\hat{p}_T^{trig}$  is the transverse momentum of the trigger particle's parent parton, and  $j_{T_y}$  is the trigger particle's transverse momentum with respect to  $\hat{p}_T^{trig}$  (likewise for the associated particle). The angle separating the trigger  $\pi^0$  and the associated hadron is  $\Delta\phi$ , and  $p_{out}$  is the perpendicular momentum component of  $p_T^{assoc}$  with respect to  $p_T^{trig}$ . The transverse momentum of the colliding partons are  $\vec{k}_T^{1,2}$ . In the case of the  $\gamma$ -hadron correlation, the direct photon is a proxy for the parent parton.

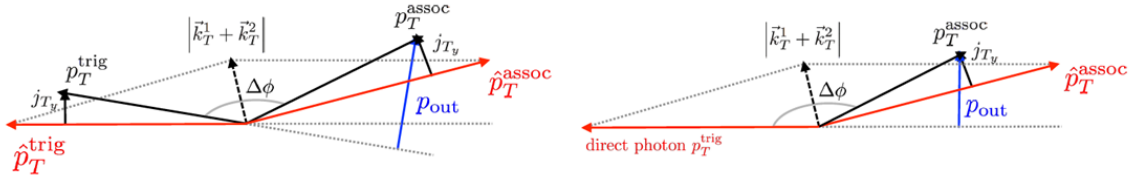


**Figure 1:** Adapted from [5]. (left) The trigger  $\pi^0$   $p_T^{trig}$  is correlated with an associated charged hadron  $p_T^{assoc}$  by the azimuthal angle  $\Delta\phi$ . (right) A direct photon is correlated with an associated charged hadron.

## 2. Experiment

The data used in this analysis were collected by the PHENIX detector at the Relativistic Heavy Ion Collider at Brookhaven National Laboratory. The PHENIX detector is shown in Fig. 2, which has two central arms each with  $\pi/2$  azimuthal coverage and  $\pm 0.35$  pseudorapidity coverage. Isolated direct photons and  $\pi^0 \rightarrow \gamma\gamma$  are detected by the electromagnetic calorimeter. Charged hadrons are detected by the drift and pad chambers. For  $p+A$  results, data are evaluated as a function of centrality, which is used as a proxy for the impact parameter. Centrality is defined by the integrated charge measured in the beam-beam counter in the direction of the heavy ion.

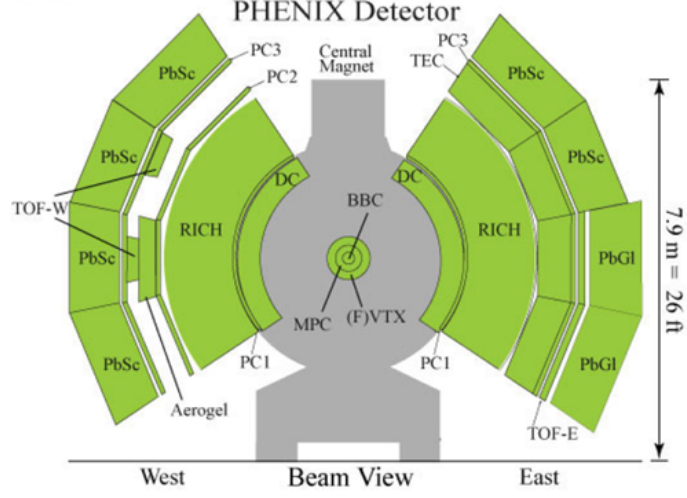


**Figure 2:** The PHENIX detector has two central arms each with  $\pi/2$  azimuthal coverage and  $\pm 0.35$  pseudorapidity coverage.

### 3. Results

Figure 3 shows the isolated direct  $\gamma$ -hadron and  $\pi^0$ -hadron  $\Delta\phi$  correlations in various  $p_T^{trig}$  and  $p_T^{assoc}$  ranges in  $p+p$  collisions at  $\sqrt{s} = 510$  GeV. This per trigger yield is:

$$\frac{1}{N_{trig}} \frac{dN}{d\Delta\phi} = \frac{1}{N_{trig}} \frac{dN/d\Delta\phi_{raw}}{dN/d\Delta\phi_{mixed} \varepsilon(p_T)} \quad (3.1)$$

where  $N_{trig}$  is the number of trigger particles,  $dN/\Delta\phi_{mixed}$  is the distribution from mixing triggered events with minimum-biased events, and  $\varepsilon(p_T)$  is the hadron detection efficiency. The near-side peak at  $\Delta\phi=0$  for  $\pi^0$ -hadrons is due to particles from the same jet, and the peak at  $\Delta\phi=\pi$  is due to the away-side charged hadrons. The effect of "trigger bias" causes the near-side peak to be larger than the away-side peak. There is no near-side peak for the  $\gamma$ -hadron correlations because yields in the photon isolation cone are physically uninterpretable. The  $\pi^0$  away-side peak is larger than the  $\gamma$  away-side peak because the  $\gamma$ -hadron correlations sample lower jet energies for a given  $p_T^{trig}$ . The underlying event contribution is the same for  $\pi^0$  and isolated direct photons as it is uncorrelated from partonic hard scattering.

The root-mean-square of  $p_{out}$  is extracted from the away-side distribution and is shown as a function of  $p_T^{trig}$  for two  $p_T^{assoc}$  ranges in the left panel of Fig. 4. The decrease of  $\sqrt{p_{out}^2}$  for  $\gamma$ -hadron is large compared to  $\pi^0$ -hadron, which may be due to the fragmentation dependence in  $\pi^0$ -hadron.

The decrease in the momentum widths for  $\pi^0$ -hadron correlations is also observed in  $p+p$ ,  $p+Al$ , and  $p+Au$  collisions at  $\sqrt{s}=200$  GeV as shown in the right panel of Fig. 4. The  $p+A$  data are measured in wide centrality ranges (0-72% for  $p+Al$  and 0-84% for  $p+Au$ ).

The  $p_{out}$  distributions for several  $p_T^{trig}$  ranges in  $p+p$  collisions at  $\sqrt{s} = 510$  GeV are shown in Fig. 5 and in  $p+Au$  collisions at  $\sqrt{s} = 200$  GeV in Fig. 6. For the  $p+p$  data, a Gaussian is fitted to the nonperturbative region ( $-1.1 < p_{out} < 1.1$ ), whereas the perturbative piece (hard gluon

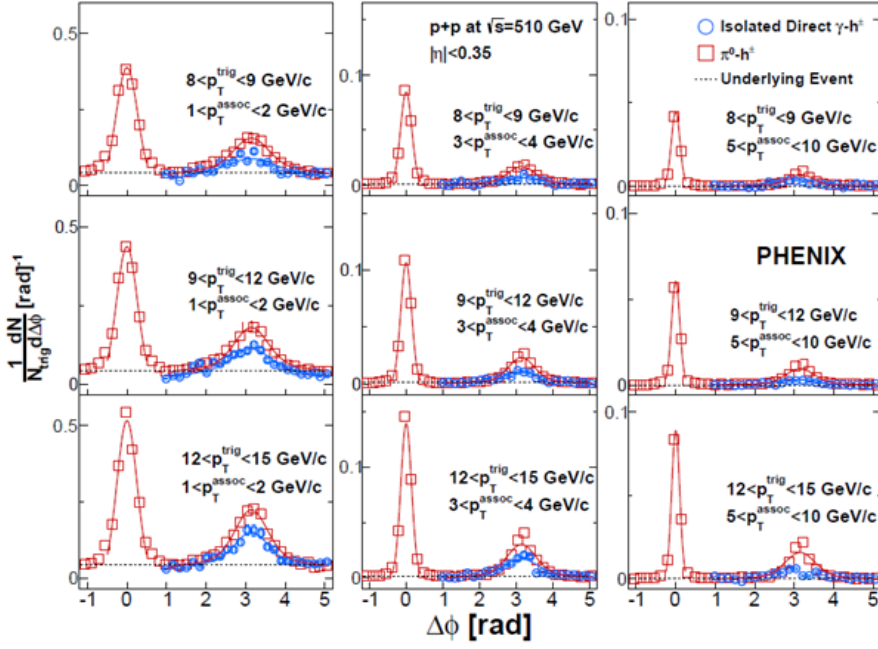


**Figure 3:**  $\pi^0$ -hadron and  $\gamma$ -hadron  $\Delta\phi$  correlations in  $p+p$  collisions at  $\sqrt{s} = 510$  GeV[5].

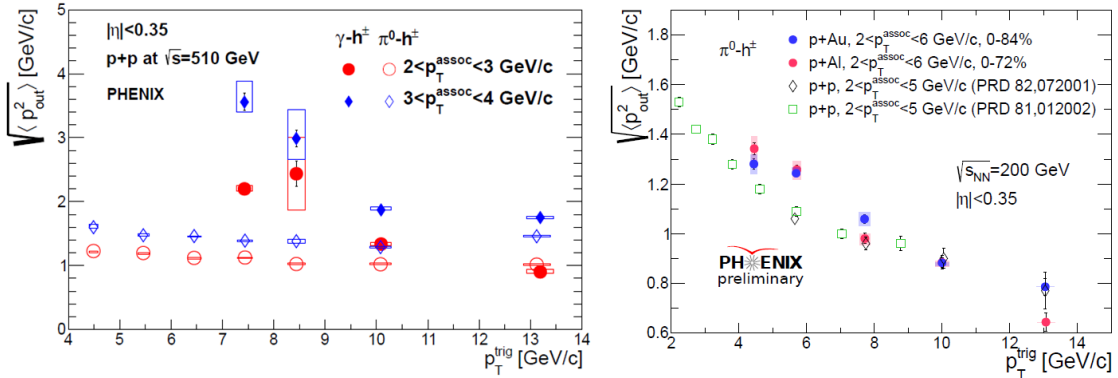


**Figure 4:** (left)  $p_{out}$  vs  $p_T^{trig}$  in  $p+p$  collisions at  $\sqrt{s} = 510$  GeV[5]. (right)  $p_{out}$  vs  $p_T^{trig}$  in  $p+p$  and  $p+A$  collisions at  $\sqrt{s} = 200$  GeV.

radiation) shows power-law behavior. A Kaplan function is used to fit the entire  $p_{out}$  range. Only the Gaussian fit is applied to the  $p+Au$  data.

The evolution of the momentum widths with hard scale can be examined in Fig. 7, where the Gaussian widths extracted from fits to the  $p_{out}$  distributions are shown as a function of  $p_T^{trig}$  in  $p+p$  collisions at  $\sqrt{s} = 510$  GeV. The decrease with  $p_T^{trig}$  is qualitatively the opposite of what has been observed in SIDIS and DY. Full event simulations using PYTHIA were used to compare the momentum widths between simulation and data. PYTHIA includes initial and final state interactions and forces all particles to color neutralize. Figure 7 shows the PYTHIA-generated widths differ by about 15%, however, the slopes are in almost perfect agreement with the data.

Figure 8 (left) compares the Gaussian widths in  $p+p$  collisions at  $\sqrt{s} = 510$  GeV with  $p+Au$

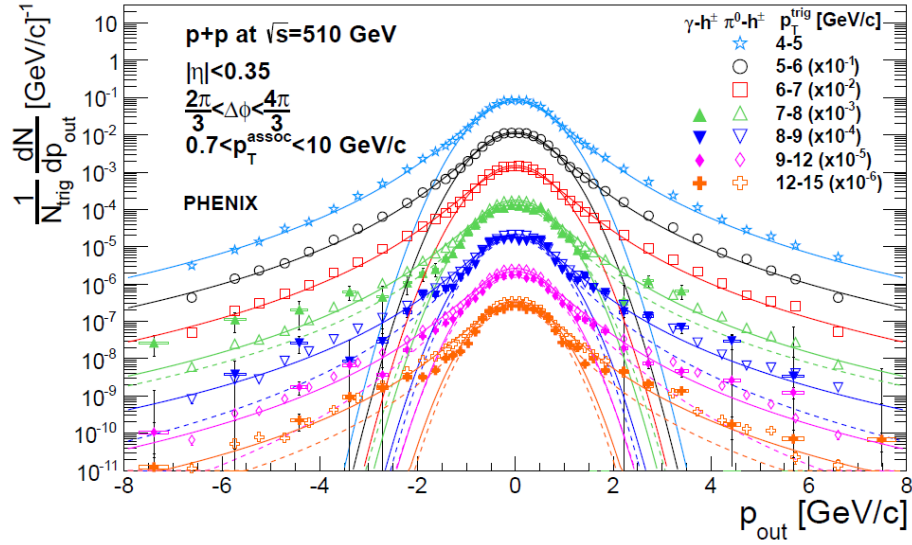


Figure 5:  $p_{out}$  distributions in  $p+p$  collisions at  $\sqrt{s} = 510$  GeV[5].

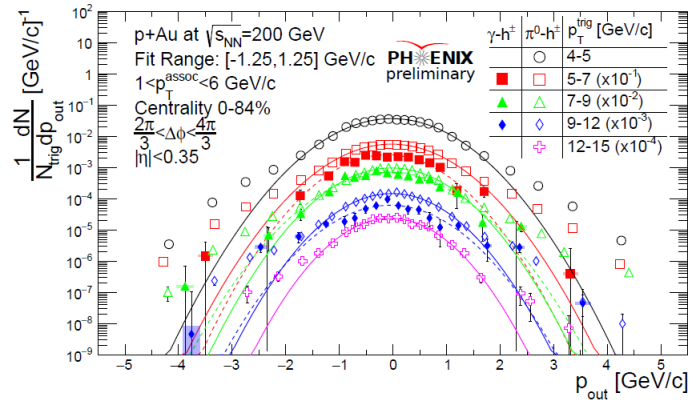


Figure 6:  $p_{out}$  distributions in  $p+A$  collisions at  $\sqrt{s} = 200$  GeV.

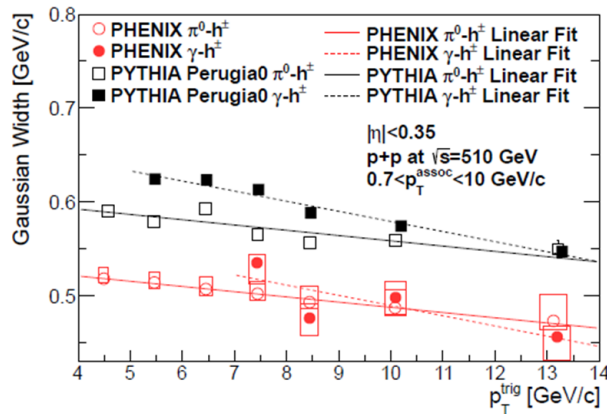
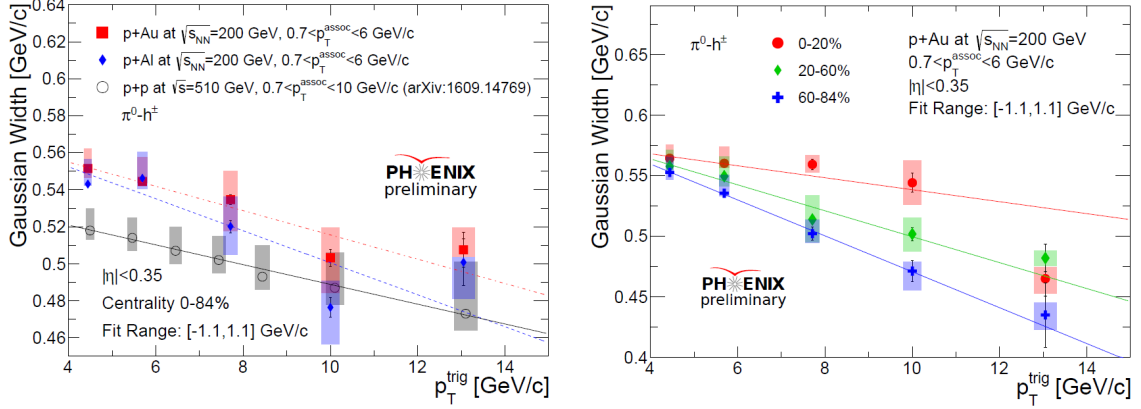


Figure 7: Gaussian widths in  $p+p$  collisions from data and simulations.

and  $p+Al$  at  $\sqrt{s} = 200$  GeV where the measurement is over 0-72% and 0-84% centrality in  $p+Al$  and  $p+Au$  data, respectively. The centrality dependence on the evolution of the Gaussian widths was also studied in Fig. 8 (right) for  $p+Au$  collisions at  $\sqrt{s} = 200$  GeV. Fits to the data for three centrality bins (0-20%, 20-60%, 60-84%) show the momentum widths to increase with increasing centrality (smaller impact parameter). The observed behavior is still under investigation, but could possibly be due to multiple scattering interactions.



**Figure 8:** (left) Gaussian widths comparison between in  $p+p$  and  $p+A$  collisions. (right) Centrality dependence on Gaussian widths in  $p+Au$  collisions.

#### 4. Conclusions

Factorization breaking is predicted in processes sensitive to nonperturbative transverse momentum effects such as  $\pi^0$ -hadron and  $\gamma$ -hadron correlations in hadronic collisions. These results show widths decrease with hard scale, suggesting possible TMD factorization breaking and color entanglement of partons across colliding protons. Examining color interactions in PYTHIA could potentially further the understanding of these results. Forthcoming results from  $p+p$  collisions at  $\sqrt{s} = 200$  GeV will give the first look at  $x_T$  scaling.

#### References

- [1] T.C. Rogers and P.J. Mulders, *Phys. Rev. D* **81** (2010) 094006.
- [2] A.V. Konychev, P.M. Nadolsky, *Phys. Lett. B* **633** (2006) 710.
- [3] C.A. Aidala, B. Field, L.P. Gamberg, and T.C. Rogers, *Phys. Rev. D* **89** (2014) 094002.
- [4] C. Adolph et al. (COMPASS Collaboration), *Eur. Phys. J.* **C73** (2013) 2531.
- [5] A. Adare et al. (PHENIX Collaboration), *Phys. Rev. D* **95** (2017) 072002.